Online ISSN 1848-3380, Print ISSN 0005-1144
ATKAFF 57(1), 76–88(2016)

Irena Galić, Časlav Livada, Branka Zovko-Cihlar

Image compression with B-tree coding algorithm enhanced by data modelling with Burrows-Wheeler transformation

DOI 10.7305/automatika.2016.07.282
UDK 004.932.057.2.021:517.95

Original scientific paper

The paper shows that the partial differential based compression framework, Edge Enhancing Diffusion Compression (EEDC) on high compression ratios can come close to or even be better than present compression standard – JPEG2000 thus presenting a novel method for image compression. In this paper EEDC will be enhanced by changing its data coding, i.e. Huffman coding will be changed with an entropy coder accompanied with Burrows-Wheeler transformation and context mixing. Images, graphs and tables show image compression results. The purpose of this article is to examine the effectiveness of the PDEs in image compression and to evaluate it by comparing to cosine and wavelet transform based compression methods.

Key words: data coder, image compression, EEDC

Kompresija slike korištenjem B-tree algoritma kodiranja poboljšana modeliranjem podataka Burrows-Wheeler transformacijom. Ovaj rad pokazuje kako je kompresija temeljena na parcijalnim diferencijalnim jednadžbama, tj. EEDC na velikom stupnju kompresije dovoljno dobra ili čak bolja od trenutačnog kompresijskog standarda – JPEG2000 time predstavljajući novu metodu kompresije slika. U ovom radu EEDC je poboljšan tako da je promijenjeno kodiranje podataka svjetline slike, tj. Huffmanovo kodiranje je zamijenjeno entropijskim koderom i Burrows-Wheeler transformacijom s miješanjem konteksta. Slike, grafovi i tablice prikazuju rezultate kompresije slika. Svrha ovog rada je ispitati efikasnost parcijalnih diferencijalnih jednadžbi u kompresiji slike te ju usporediti metodama kompresije koje su bazirane na kosinusnoj i wavelet transformaciji.

Ključne riječi: kodiranje podataka, kompresija slike, EEDC

1 INTRODUCTION

The purpose of this paper is to investigate the possibility of compressing images better than the current compression standards, the JPEG 2000 and JPEG lossy coder. The JPEG coder works by using the discrete cosine transform or DCT and JPEG 2000 coder is using the DWT or discrete wavelet transform. Both perform on various compression ratios so in order to achieve better compression, a novel approach to image compression must be used. In this research partial differential equations (PDEs) are discussed and explained because the PDEs are nowadays successfully applied to problems in image denoising, enhancement, inpainting, segmentation and also image compression [6, 7, 10, 14].

The PDE image compression model used in this research is based on EEDC lossy image compression (Edge Enhancing Diffusion Compression). EEDC is using the BTTC (Binary Tree Triangular Coding) in which the quadratic image is decomposed into triangles and stored in a binary tree structure thus compressing the image. The structure of the tree and the nodes (vertices of the triangles) are sent to the decoder in order to decompress the image. To acquire the image, it has to be interpolated from the vertices by a selected interpolation method. These methods, i.e. smoothing operators will be explained in the forthcoming text. The EEDC coder is using the Edge Enhancing Diffusion as its interpolation method for creating the image.

The PDE based compressions method name presented in this paper is EEDC-BWT. It is based on EEDC with major enhancement in the binary tree compression (compression of the tree structure and the vertices that contain the grayvalues of the image). Second part of the name "BWT" comes from the Burrows-Wheeler transformation that is used in the process of binary tree structure compression. Thus giving more space to store the valuable grayvalues contained in vertices of the triangles, i.e. the more vertices we store, the more detailed image can be interpolated. With more points for interpolation the restored image will have better objective and subjective scores than the current

standards, JPEG and JPEG 2000 and that is the original scientific contribution of this paper. Similar research was performed in [9] but in this research the extreme possibilities of the Burrows-Wheeler transform were tested, context mixing was not so detailed examined because the latter research showed it did not have so great impact on the compression itself. Also the subjective quality measurement is added to this paper.

The basic idea of PDE-based interpolation will be described in the following section. Afterwards the new compression model and its compression results will be presented and compared to EEDC [6], JPEG [12] and JPEG 2000 [16].

2 PDE-BASED INTERPOLATION

Firstly, a general model for PDE-based image interpolation will be described, then a number of options for smoothing operators will be investigated, and finally an experiment that illustrates their performance will be presented.

2.1 General model

Let $\Omega \subset R^n$ denote an n-dimensional image domain and the goal is to recover some unknown scalar-valued function $v : \Omega \to R$, from which only its values on some subset $\Omega_1 \subset \Omega$ are known. The goal is to find an interpolating function $u : \Omega \to R$ that is smooth and close to v in $\Omega \backslash \Omega_1$ and identical to v in Ω_1.

The evolution is initialised with some function $f : \Omega \to R$ that is identical to v on Ω_1 and the following evolution is considered

$$\partial_t u = (1 - c\,(x))\, Lu - c\,(x)\,(u - f) \tag{1}$$

with $u(x, 0) = f(x)$ and reflecting boundary conditions on the image boundary $\partial\Omega$. The function $c : \Omega \to R$ is the characteristic function on Ω_1 and L is some elliptic differential operator. The idea is to solve the steady state equation

$$(1 - c\,(x))\, Lu - c\,(x)\,(u - f) = 0 \tag{2}$$

with reflecting boundary conditions. This elliptic PDE can be regarded as the steady state of the evolution equation

$$\partial_t u = Lu \tag{3}$$

with Dirichlet boundary conditions given by the interpolation data on Ω_1.

2.2 Specific smoothing operators

Regarding the elliptic differential operator L, many possibilities exist. The simplest and the best investigated one uses the Laplacian leading to *homogeneous diffusion* [8]:

$$\partial_t u = \Delta u. \tag{4}$$

A prototype for a higher order differential operator is the biharmonic operator giving the *biharmonic smoothing* evolution

$$\partial_t u = -\Delta^2 u. \tag{5}$$

Using it for interpolation comes down to thin plate spline interpolation [5].

The multidimensional generalisation of quintic spline interpolation leads to *triharmonic smoothing*:

$$\partial_t u = \Delta^3 u. \tag{6}$$

Note that only the second-order differential operators allow a maximum–minimum principle, where the values of u stay within the range of the values of f in Ω_1.

A second order PDE that has been advocated for interpolation purposes [11] is given by the *absolute monotone Lipschitz extension* (AMLE) model:

$$\partial_t u = \partial_{\eta\eta} u. \tag{7}$$

Nonlinear isotropic diffusion processes with their corresponding PDE formulation was first given by Perona and Malik [13]

$$\partial_t u = div\left(g\left(|\nabla u|^2\right)\nabla u\right) \tag{8}$$

and it uses diffusivity such as

$$g\left(s^2\right) = \frac{1}{1 + s^2/\lambda^2} \tag{9}$$

with some contrast parameter $\lambda > 0$ that separates forward and backward diffusion areas. Nonlinear isotropic diffusion with Perona-Malik diffusivity (8) is effective at removing noise and preserving edges, but can create false edges as well as a blocky appearance in the smoothed image.

A higher-order version of the Perona-Malik equation (7) reduces large jumps in intensity. You and Kaveh [19] introduced a *nonlinear fourth-order isotropic diffusion*

$$\partial_t u = \Delta\left(g\left(\left(\Delta u\right)^2\right)\Delta u\right) \tag{10}$$

The fourth-order method results in image intensity functions with jumps in gradient, but this is far less obvious to the human eye.

Real anisotropic behaviour is possible when a diffusion tensor is used. As a prototype for nonlinear anisotropic diffusion filtering *edge-enhancing diffusion* (*EED*) [17] is considered and the idea is to reduce smoothing across edges while still permitting diffusion along them. The elliptic differential operator for EED diffusion is governed by

$$\partial_t u = div\left(g\left(\nabla u_\sigma \nabla u_\sigma^T\right)\nabla u\right). \tag{11}$$

2.3 Comparison of specific smoothing operators

In order to evaluate the before mentioned PDEs for scattered data interpolation a discretisation with central finite differences in space is used. For AMLE, nonlinear isotropic diffusion Perona-Malik diffusivity, nonlinear fourth-order isotropic diffusion, biharmonic and triharmonic smoothing an explicit scheme was used whereas for homogeneous diffusion, nonlinear isotropic diffusion Charbonnier diffusivity and edge-enhancing diffusion we performed a semi-implicit time discretisation with SOR as solver for linear systems of equations.

Figure. 1 contains results that illustrate the use of the different smoothing operators for scattered data interpolation. It presents a standard test image trui of size 256x256 pixels, where 2 percent of all pixels have been chosen randomly as scattered interpolation points. It is evident that homogeneous diffusion is not suitable for scattered data interpolation, since it creates singularities at the interpolation points. Use of biharmonic smoothing gives fairly good results, but suffers from overshoots and undershoots near edges (see e.g. the scarf). Despite many favourable theoretical properties [11], AMLE does not live up to its expectations; result seems to contain isolated blurry white or black pixels near edges.

Transfer from homogeneous diffusion to nonlinear isotropic diffusion does not give an improvement. especially for Perona-Malik diffusivity. Charbonnier diffusivity gives better result for nonlinear isotropic diffusion, although linear grey value transitions are oversegmented in constant stairs and tend to keep many interpolation points as isolated singularities. Nonlinear fourth-order isotropic diffusion with Charbonnier diffusivity suppreses staircasing, however, contains a lot of speckle artefacts. The fact that EED gives the best results shows the importance of the anisotropic behaviour. Its ability to smooth along edges seems to be very beneficial for avoiding singularities at interpolation points. This second-order PDE respects a maximum–minimum principle, such that the solution is within the grey scale bounds of the interpolation points.

The results have been optimised in order to minimise the l^1 -error. A quantitative error analysis is given in Table 1, where the *average absolute error* (AAE) is computed between the interpolated image $(u_{i,j})$ and the original image $(v_{i,j})$:

$$AAE = \frac{1}{N} \sum_{i,j} |u_{i,j} - v_{i,j}| \,, \tag{12}$$

where N denotes the number of pixels. Smaller AAE means smaller difference of decoded and original image. At locations where overshoots and undershoots occur, i.e. where they lead grey values outside the interval [0, 255],

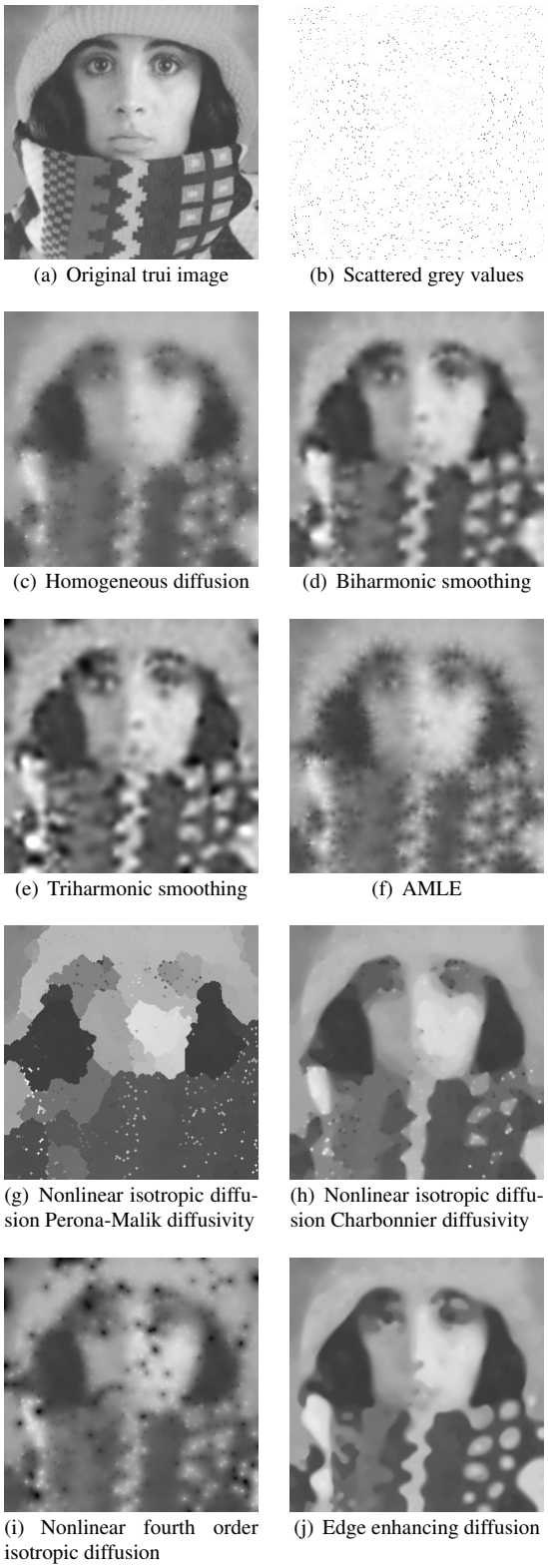

(a) Original trui image (b) Scattered grey values

(c) Homogeneous diffusion (d) Biharmonic smoothing

(e) Triharmonic smoothing (f) AMLE

(g) Nonlinear isotropic diffusion Perona-Malik diffusivity (h) Nonlinear isotropic diffusion Charbonnier diffusivity

(i) Nonlinear fourth order isotropic diffusion (j) Edge enhancing diffusion

Fig. 1. Scattered data interpolation

they have been truncated. Our experiments show that the average absolute error gives a ranking that corresponds well with our visual impression. These disclosures are in accordance with results from [17] where EED proved to be the PDE of choice for interpolation tensor data. Therefore, our focus will be EED and all optimisations of the approximation quality will be carried out with respect to the average absolute error.

Table 1. Average absolute errors (AAE) for the PDEs used for scattered data interpolation in Fig. 1.

PDE method	***AAE***
homogeneous diffusion	14.52
biharmonic smoothing	10.44
triharmonic smoothing	13.49
AMLE	14.85
nonlinear isotropic diffusion Perona-Malik diffusivity	24.63
nonlinear isotropic diffusion Charbonnier diffusion	11.76
nonlinear second order Charbonnier diffusion	21.30
edge-enhancing diffusion	9.23

Even when the mask is just a simple grid of grey values, EED interpolation gives fairly good results as it can be seen on Fig. 2. Every 7th pixel is stored and still the 2% of pixels are preserved as sparse interpolation points. The average absolute error for reconstructed image is 7.39 which is quite good since we used a simple grid to save our grey values.

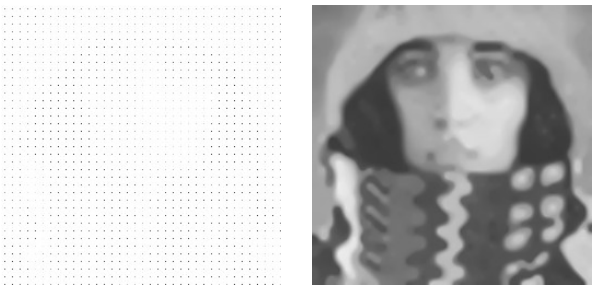

(a) Sparse image (b) Interpolated image

Fig. 2. Mesh interpolation

3 EEDC-BWT CODER

In this section, a clear overview of the proposed method coder is explained. A detailed block scheme can be seen on Fig. 3.

The EEDC-BWT coding scheme consists of three main parts; triangle decomposition process, Burrows-Wheeler transform and range coding. The input in the first block at Fig. 3.a) is the selected grayscale image. First block performs the triangle decomposition process that will be explained in the following text as BTTC. The output of the first block are two binary strings, one containing the binary tree structure and the second one containing the grayvalues. Information for the decoder in order to successfully reconstruct the image is also provided. Detailed explanation of the whole process is described in the subsection 3.2. In order to save more space for the crucial vertices needed for the interpolation and image reconstruction, a more sophisticated compression method is needed. The classic entropy coders like Huffman and arithmetic coding did not suffice to the challenge so a range coder is tested. However it did not perform well until a modified input was sent to its coder. In order to prepare the input stream for the range coder shown at Fig. 3.c), Burrows-Wheeler transform is used (Fig. 3.b)). Since the coded input is a stream of grayvalues of the scattered vertices, the Burrows-Wheeler transform reorders them in order for the entropy coder to take advantage of the regularities in the new-formed stream. The last step is the coding of the grayvalues (values from 0 – 255) using an entropy coder. The used coder, range coder is similar to arithmetic coding but uses integer logic instead of floating point logic. Burrows-Wheeler transform and range coding are explained in subsection 3.3.

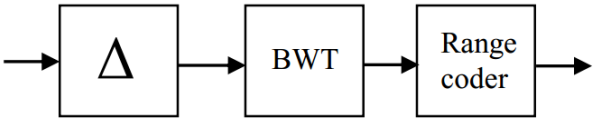

Fig. 3. EEDC-BWT block diagram

In order to reconstruct the image from the scattered data, an interpolation is needed. The interpolation methods are described in section 2 and as a conclusion edge-enhancing diffusion is selected due to its lowest AAE score. Edge Enhancing Diffusion is useful for scattered data interpolation and this method can be used for image reconstruction [6, 7]. For compression purposes interpolation quality is not enough if the image data is too expensive to encode.

3.1 Binary tree triangular coding

In B-tree triangular coding, an image is decomposed into a number of triangular regions that can be recovered in good quality by interpolation from the vertices [1, 7]. The decomposition into triangles is stored in a binary tree structure. The image is split by one of its diagonals into two triangles, as shown on Fig. 4.

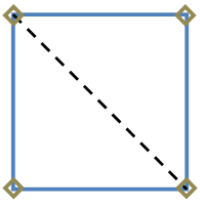

Fig. 4. First step of BTTC algorithm

To refine this initial configuration, an approximation $(u_{i,j})$ of the image $(f_{i,j})$ is calculated by using only the grey values from the vertices and interpolating rest of image. If the error $e_{i,j} = |u_{i,j} - f_{i,j}|$ satisfies $e_{i,j} < \varepsilon$ where $\varepsilon > 0$ for image, the representation by triangles is considered good. Otherwise the triangle is split into two similar triangles by the height on its hypotenuse. The centre of the hypotenuse becomes an additional vertex.

Approximation errors recalculation within the new triangles determines whether to split these again or not as shown on Fig. 5.

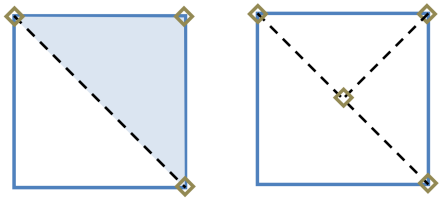

(a) Triangle reconstruction via interpolation

(b) Splitting of the unsatisfactionary reconstructed triangle

Fig. 5. Mesh interpolation

3.2 Coding the Binary tree

Each triangle in the splitting process is represented by a node while leaves correspond to those triangles which are not divided further. When a triangle is split, its two sub triangles become the children of its representing node. To store the structure of the tree, the tree needs to be traversed. For a node that has children 1 is stored, and a 0 for a node without children, i.e. a leaf. Further space in storing the tree is saved by measuring minimal and maximal depth of the tree. Only for nodes between the minimal and maximal depth of the tree, bits are stored. Splitting process is shown on Fig. 6. Coding the grey values in all vertices starts by zig-zag traversal of sparse image created with the binary tree structure and storing it in a sequence of grey values. The main difference between EEDC in [7] is in the grey value coder. EEDC uses Huffman coding for coding of the grey values. First, data modelling is applied in the form of Burrows-Wheeler transform and then the changed sequence is coded with the range coder that uses context mixing algorithm.

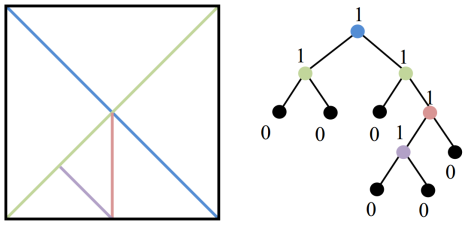

(a) Decomposition of image on triangular areas

(b) Binary tree structure

Fig. 6. Triangle splitting process

Figure 7. shows image decomposed on triangles by following the rules in triangle splitting process mentioned before. Fig. 6. clearly shows that the most triangles are in the areas with high details like eyes, nose, mouth and some areas on the scarf. Coded image format consist of these elements:

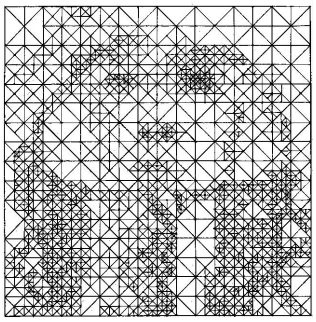

Fig. 7. Triangle decomposition

- image width and height
- minimal and maximal binary tree depth
- binary string encoding binary tree structure (1 bit for each node between minimal and maximal depth, filled up with zeros to the next byte boundary)
- binary string encoding grey values using BWT and range coder with context mixing

3.3 Coding the grey values

In this part, the grey value data transformer and encoder will be described. First the input sequence is prepared for the range coder by means of applying Burrows-Wheeler transformation. After that, range coder with implemented context mixer is applied on the transformed sequence.

3.3.1 BWT Basics

BWT is an algorithm that rearranges a block of data using a sorting algorithm. The resulting output block contains exactly the same data elements that it started with only one difference, their ordering. The transformation is reversible, meaning that the original ordering of the data elements can be faithfully restored [12].

The BWT is performed on an entire block of input data at once. One of the effects of BWT is produce strings of identical symbols than those found in the original data. BWT will be described with an example in the following text and commented with explanatory pictures respectively. BWT algorithm consists of four steps:

- Read in input data: bcdaca, N = 6

$$C_0 = \text{`}b\text{'}, C_1 = \text{`}c\text{'}, C_2 = \text{`}d\text{'}, C_3 = \text{`}a\text{'},$$

$$C_4 = \text{`}c\text{'}, C_5 = \text{`}a\text{'}$$

- Think of the block as a cyclic buffer and N rotations (strings) $S_0, \ldots, S_{N-1}$ can be constructed such that

$$S_0 = C_0, \ldots, C_{N-1}$$

$$S_1 = C_1, \ldots, C_{N-1}, C_0$$

$$S_2 = C_2, \ldots, C_{N-1}, C_0, C_1$$

$$S_{N-1} = C_{N-1}, C_0, \ldots, C_{N-2}$$

- Lexicographically sorting of $S_0, \ldots, S_{N-1}$ which yields in:

$$\begin{array}{ll} S_0 = \text{`}bcdaca\text{'} & S_5 = \text{`}abcdac\text{'} \\ S_1 = \text{`}cdacab\text{'} & S_3 = \text{`}acabcd\text{'} \\ S_2 = \text{`}dacabc\text{'} & S_0 = \text{`}bcdaca\text{'} \\ S_3 = \text{`}acabcd\text{'} \quad \Rightarrow & S_4 = \text{`}cabcda\text{'} \\ S_4 = \text{`}cabcda\text{'} & S_1 = \text{`}cdacab\text{'} \\ S_5 = \text{`}abcdac\text{'} & S_2 = \text{`}dacabc\text{'} \end{array}$$

- Output the string L, consisting of the last character in each of the rotations in their sorted order along with I, the sorted row containing S_0

$$L = \text{`}cdaabc\text{'}, I = 2$$

The string of last characters (L) along with the row S_0 is enough information to reconstruct the original block (S_0).

3.3.2 Range coding

Range coder is a technique of conversion of sequences to a single integer. Range coder is similar to arithmetic coder with only one difference, all fractions are brought to common denominator [14]. Algorithm takes whole sequences of bits and transforms them into integers, depending on their known statistical properties.

The range coding algorithm is as follows:

- Divide interval [0, 1] into M intervals that correspond to symbols, symbol length is proportional to symbols probability.
- Select the interval of the first symbol in queue.
- Subdivide the current symbol interval into new M subintervals, proportional to their probabilities.
- From these subintervals, select one that matches the next symbol in queue.
- Repeat steps 3 and 4 until all symbols are coded.
- Output the interval value in binary form.

Let's take for example that the picture has 10000 elements. Statistical analysis gave following element frequencies:

A : 200, B : 300, C : 100, D : 300, E : 300, F : 500,

G : 600, H : 200

Probabilities are as follows:

P(A) = 0.08, P(B) : 0.12, P(C) : 0.04, P(D) : 0.12,

P(E) : 0.12, P(F) : 0.2, P(G) : 0.24, P(H) : 0.08.

Figure 8. shows range coding process. Range coding is similar to arithmetic coding so it would not yield good results as stated in [6] so we apply context mixing algorithm to improve compression.

Context mixing is an algorithm in which the next symbol predictions of two or more statistical models are combined to yield a prediction that is often more accurate than any of the individual predictions [18]. If we don't use context mixing to know the probabilities of the input data, we would notice that most of symbols have same probability therefore no compression would be achieved. Using a higher order context mixing on context sensitive input data makes probabilities more skewed. Two general approaches of context mixing can be used:

- Linear mixing uses a weighted average of the predictions weighted by evidence
- Logistic mixing first transforms the predictions into logistic domain before averaging

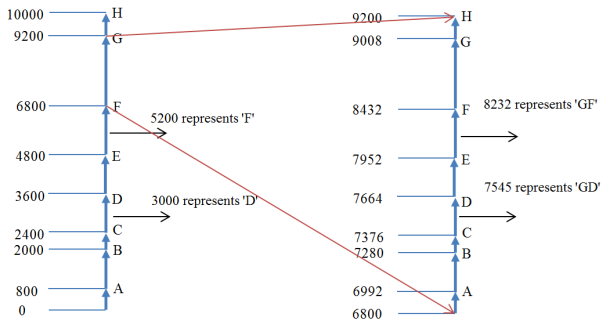

Fig. 8. Range coding process example

4 OBJECTIVE AND SUBJECTIVE IMAGE QUALITY MEASUREMENT

Objective digital image quality evaluation is based on differences of the original and decoded images which depicts the quality loss. Numerous methods for image quality assessment that differ in approach, complexity and accuracy have been developed. Digital image can be represented by a two dimensional matrix whose elements present grey values. Apart from before mentioned AAE (12), the following methods are used for image quality measurement.

Mean Square Error (MSE):

$$MSE = \frac{1}{N} \sum_{i,j} |u_{i,j} - v_{i,j}|^2 \tag{13}$$

MSE is a measure of noise power. Square of the error attenuates small differences between two pictures but increases big differences. Smaller values of MSE mean smaller error, i.e. smaller differences of decoded and original image.

Signal to Noise Ratio (SNR):

$$SNR(f,g) = 10 \cdot \log_{10} \left(\frac{\sigma^2(g)}{MSE} \right) \tag{14}$$

SNR is a ratio of the average signal strength and average strength of present noise, i.e. in this case differences from the original picture. Bigger value of SNR means bigger similarity with the original image.

The amplitude of picture elements has a range MAX, where q is the number of bits needed to display the amplitude of the original image elements. MSE does not take into account the MAX, therefore we introduce

Peak Signal to Noise Ratio (PSNR):

$$\begin{aligned} PSNR(u,v) &= 10 \cdot \log_{10} \left(\frac{MAX^2}{MSE} \right) \\ &= 20 \cdot \log_{10} \left(\frac{MAX}{MSE} \right) \end{aligned} \tag{15}$$

PSNR is the logarithmic ration between the maximum signal strength and noise strength. Unit of measure is decibel (dB). The value of PSNR = 0 means there is no similarity between the tested pictures, while value of PSNR = 100 means that the two pictures are identical.

Subjective quality measurement used in this research is based on Double stimulus impairment scale. Double stimulus method represents categorical rating, in which observers judge the quality of a pair of images on a fixed 5-point scale. It involves displaying a reference image and a test image in a random order one after another for 3 seconds each with a pause of 1.5 seconds between images. After that, a voting screen is displayed on which both images are assessed separately using the one of the five categories: excellent, good, fair, poor or bad. Subjective analysis was performed on test subjects in an controlled environment.

5 EXPERIMENTAL RESULTS

Results of compression method explained in this article (Burrows-Wheeler Transform + Range Coding + Context Mixing or shorter EEDC-BWT) will be compared to EEDC [6], JPEG and JPEG2000 on four images of 257x257 elements. Compression was done on five different degrees of compression: 0.8, 0.4, 0.2, 0.1 and 0.05 bpp. Four test images are shown of Fig. 9. JPEG coder could not perform the compression ratio at 0.05 bpp so that data is missing.

By observing and analysing data from the Table 2. we can conclude that the EEDC-BWT compression is better than its predecessor, the EEDC. AAE value increases with the compression ratio increase. EEDC-BWT is the best codec, by judging the AAE parameter, among four tested in high compression, i.e. at 0.1 and 0.05 bpp. Compression of image trui at 0.1 bpp is shown on Fig. 11. We can see that area around the eyes is clearer and borders are more visible. The details on the scarf are more defined, i.e. the pattern is clearer.

The direct improvement in the quality of the picture can be seen by observing the AAE parameter. Fig. 10 shows the improvement between EEDC and EEDC-BWT in percentages for every compression ratio for image trui.

We can conclude that the best improvement is at the compression rates of 10:1 and 160:1, i.e. at 0.8 and 0.05 bpp.

As for the subjective quality measurement, the results are given in the Table 3. We can conclude that the worst overall score was achieved by JPEG at all compression ratios. Our novel method achieved better results than the JPEG 2000 at high compression ratios where the wavelet artefacts were accentuated.

The AAE parameter in the cameraman image compression is, again, the best at 0.1 bpp as shown on Fig. 13. We

Table 2. Objective evaluation for image trui

	Trui							
	AAE				***MSE***			
bpp	***JPEG***	***EEDC***	***JPEG 2000***	***EEDC-BWT***	***JPEG***	***EEDC***	***JPEG 2000***	***EEDC-BWT***
0.8	2.24	2.52	1.97	2.44	9.54	10.89	6.71	10.24
0.4	4.12	3.41	3.04	3.37	32.06	21.71	18.10	21.35
0.2	11.25	5.00	4.84	4.98	216.59	51.54	46.16	50.88
0.1	33.65	7.55	7.72	7.48	1400.2	134.09	119.94	132.45
0.05		10.49	13.53	10.22		245.14	349.34	242.46
	SNR				***PSNR***			
bpp	***JPEG***	***EEDC***	***JPEG 2000***	***EEDC-BWT***	***JPEG***	***EEDC***	***JPEG 2000***	***EEDC-BWT***
0.8	24.09	23.58	25.67	24.56	38.34	37.76	39.87	38.12
0.4	18.85	20.52	21.33	21.13	33.07	34.76	35.55	34.88
0.2	10.75	16.72	17.21	16.99	24.77	31.01	31.49	31.12
0.1	4.07	12.43	12.98	12.53	16.67	26.86	27.34	27.00
0.05		9.64	8.09	10.00		24.24	22.70	24.35

(a) Trui

(b) Cameraman

(c) Boats

(d) Office

Fig. 9. Test images

Table 3. Subjective evaluation for image trui

bpp	***JPEG***	***JPEG 2000***	***EEDC-BWT***
0.8	4.28	4.79	4.75
0.4	3.09	4.23	3.52
0.2	2.17	2.90	2.98
0.1	1.38	1.75	1.61
0.05		1.17	1.49

can clearly see that the legs of the tripod are more detailed and also the background is richer. The JPEG2000 codec is

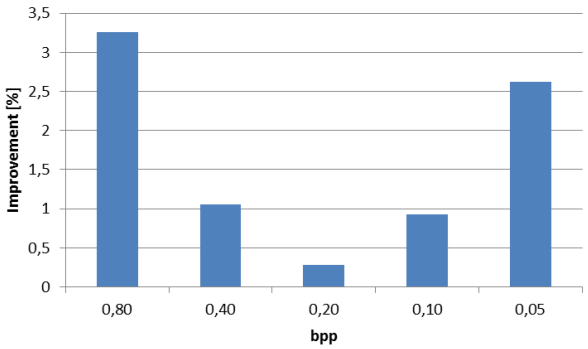

Fig. 10. EEDC-BTW versus EEDC improvement for image trui

good for high details which can be seen on tripod but the image is a bit blurry.

Figure 12. shows the EEDC compression methods improvement in percentages for the image cameraman. We can see that the general improvement is at high compression ratios, i.e. 80:1 and 160:1 (0.1 bpp and 0.05 bpp). According to the results in the Table 5. we can conclude that for the image Cameraman EEDC-BWT method comes close to the JPEG 2000 in term of the subjective quality. JPEG falls short for other two compression methods but is only better than the EEDC-BWT at 0.8 bpp.

Figures 15. and 17. show images with high amount of details and the effect of every compression method. Figure 15. shows the boats image which is high detailed. We can see that at the sea, on the ship and especially on the ropes in the top right corner. The JPEG2000 codec is, from far, very good in this picture but again it has that blurry overlay. By comparing the two EEDC algorithms, we can see that the BWT is a little better in the details on the boat, in the

Table 4. Objective evaluation for image cameraman

	Cameraman							
	AAE				***MSE***			
bpp	***JPEG***	***EEDC***	***JPEG 2000***	***EEDC-BWT***	***JPEG***	***EEDC***	***JPEG 2000***	***EEDC-BWT***
0.8	4.45	4.79	3.51	4.78	50.94	62.44	25.30	41.56
0.4	6.74	7.00	5.53	7.10	120.64	153.93	75.69	151.49
0.2	13.97	9.32	8.07	9.31	380.96	290.50	179.32	293.59
0.1	29.46	11.29	11.33	11.19	1320.1	456.88	349.99	446.16
0.05		13.98	16.40	13.88		720.39	732.88	709.86
	SNR				***PSNR***			
bpp	***JPEG***	***EEDC***	***JPEG 2000***	***EEDC-BWT***	***JPEG***	***EEDC***	***JPEG 2000***	***EEDC-BWT***
0.8	18.79	17.83	21.92	17.91	31.06	30.18	34.10	30.22
0.4	14.97	13.80	17.09	13.80	27.32	26.26	29.34	26.19
0.2	9.63	10.88	13.22	10.99	22.32	23.50	25.60	23.45
0.1	4.00	8.75	10.19	8.80	16.93	21.53	22.69	21.34
0.05		6.48	6.40	6.83		19.56	19.48	19.62

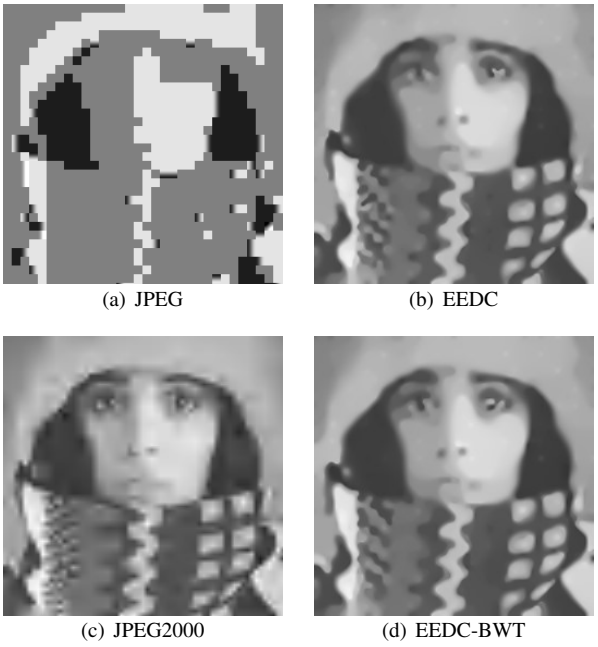

(a) JPEG (b) EEDC

(c) JPEG2000 (d) EEDC-BWT

Fig. 11. Trui image compression

Table 5. Subjective evaluation for image cameraman

bpp	***JPEG***	***JPEG 2000***	***EEDC-BWT***
0.8	4.91	4.95	4.75
0.4	3.33	4.26	4.24
0.2	3.06	3.19	3.32
0.1	2.15	2.27	2.28
0.05		1.22	1.17

sky and especially in the top right corner, i.e. the ropes.

Tables 6. and 8. follow the pictures with statistical data

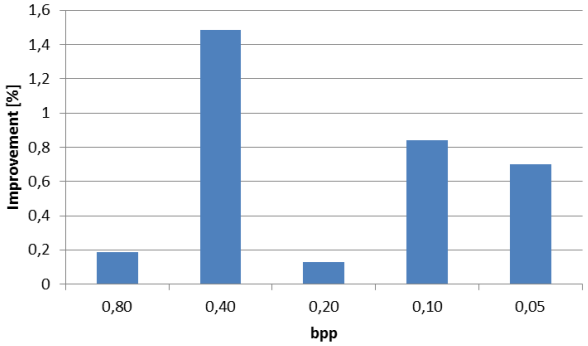

Fig. 12. EEDC-BTW versus EEDC improvement for image cameraman

for images boats and office and tables 7. And 9. show the results of the subjective analysis.

Figure 14. shows the improvement in percentages when the BWT transform is added to EEDC. We can see that the improvement is best at the 10:1 compression ratio, i.e. at 0.8 bpp. The areas which interest us (0.2, 0.1 and 0.05 bpp) are quite close to each other.

Again, the JPEG is graded as the worst coder. The novel compression method performs the best at 0.05, 0.1 and 0.2 bpp but at low compression rations, the JPEG 2000 is graded as the best.

Figure 16 shows the EEDC-BWT improvement that was achieved with using this compression method for image office. We can clearly see that this algorithm has the best improvement among all other images.

Its record is at 0.2 bpp and gives 32% improvement to EEDC. The high compression ratio cases are not quite as the low to mid compression ratios but still are good (3-4%).

Table 6. Objective evaluation for image boats

	Boats							
	AAE				***MSE***			
bpp	***JPEG***	***EEDC***	***JPEG 2000***	***EEDC-BWT***	***JPEG***	***EEDC***	***JPEG 2000***	***EEDC-BWT***
0.8	5.42	6.58	4.39	6.12	61.14	94.55	35.64	93.12
0.4	8.08	25.25	6.66	24.99	133.88	185.48	88.69	182.32
0.2	15.03	11.82	9.28	11.53	394.12	306.50	177.55	301.15
0.1	25.81	14.39	11.98	14.12	1069.9	461.09	308.98	459.68
0.05		17.19	15.94	16.93		696.31	546.96	686.22
	SNR				***PSNR***			
bpp	***JPEG***	***EEDC***	***JPEG 2000***	***EEDC-BWT***	***JPEG***	***EEDC***	***JPEG 2000***	***EEDC-BWT***
0.8	15.32	12.82	17.71	13.32	30.27	28.21	32.61	28.34
0.4	11.86	9.85	13.64	10.44	26.86	25.33	28.65	25.41
0.2	7.24	7.79	10.52	7.98	22.18	23.27	25.64	23.40
0.1	2.76	5.82	7.81	5.98	17.84	21.49	23.23	21.50
0.05		3.70	4.71	4.10		19.70	20.75	19.81

(a) JPEG (b) EEDC

(c) JPEG2000 (d) EEDC-BWT

Fig. 13. Cameraman image compression

Table 7. Subjective evaluation for image cameraman

bpp	***JPEG***	***JPEG 2000***	***EEDC-BWT***
0.8	4.49	4.95	4.88
0.4	3.00	4.12	3.44
0.2	2.52	2.22	2.87
0.1	1.28	2.01	1.85
0.05		1.05	1.20

With the EEDC compression method we don't even see that the image represents office, whereas with the EEDC-BWT we can see the windows, a desk and even some things on the desk like personal computer, etc. The window structure can be seen but it is a bit blurry.

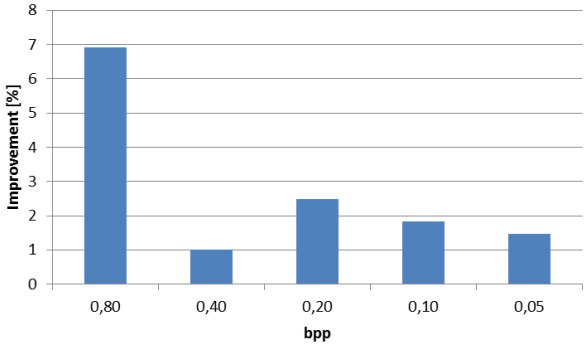

Fig. 14. EEDC-BTW versus EEDC improvement for image boats

The compression of the boats image, at 0.1 bpp, is not best in the case of EEDC-BWT but in the case of JPEG2000 codec that is superior to all three other compression methods. This can be explained by large high detail areas that seem to be the problem for EEDC and EEDC-BWT. This case is also present at the picture office where the EEDC-BWT is, even on this small scale, visually better that the predecessor. Again, fine detail makes JPEG2000 the best codec for this picture.

Subjective analysis implies that the JPEG codec is by far the worst codec for this kind of high-rate compression. Because of the high detail in the image, at high compression ratios.

Table 8. Objective evaluation for image office

	Office							
	AAE				***MSE***			
bpp	***JPEG***	***EEDC***	***JPEG 2000***	***EEDC-BWT***	***JPEG***	***EEDC***	***JPEG 2000***	***EEDC-BWT***
0.8	2.89	5.12	2.09	4.32	20.03	76.32	8.79	37.29
0.4	5.82	8.88	4.11	7.21	78.41	205.17	37.61	123.70
0.2	15.85	11.07	7.40	7.61	503.47	304.33	128.17	137.49
0.1	27.76	16.26	13.01	15.74	1242.4	695.93	383.95	682.21
0.05		22.37	21.67	21.97		1243.3	994.25	1290.1
	SNR				***PSNR***			
bpp	***JPEG***	***EEDC***	***JPEG 2000***	***EEDC-BWT***	***JPEG***	***EEDC***	***JPEG 2000***	***EEDC-BWT***
0.8	23.71	18.36	27.39	20.93	35.11	31.19	38.69	32.41
0.4	17.78	14.22	21.04	15.62	29.19	25.12	32.38	27.21
0.2	9.57	11.53	15.61	15.16	21.11	23.30	27.05	26.75
0.1	5.81	7.72	10.53	7.96	17.19	19.71	22.29	19.79
0.05		4.96	5.86	4.89		17.19	18.16	17.02

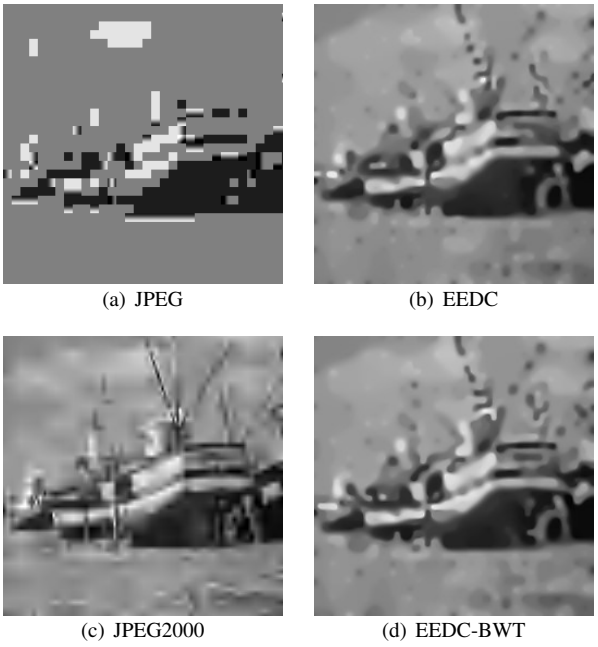

(a) JPEG (b) EEDC

(c) JPEG2000 (d) EEDC-BWT

Fig. 15. Boats image compression

Table 9. Subjective evaluation for image office

bpp	***JPEG***	***JPEG 2000***	***EEDC-BWT***
0.8	4.49	4.95	4.88
0.4	3.00	4.12	3.44
0.2	2.52	2.22	2.87
0.1	1.28	2.01	1.85
0.05		1.05	1.20

6 CONCLUSION

This article has proved that the use of entropy coders, i.e. range coding can also be good for high-rate image compression. Reduction of the AAE parameter, which is a direct image quality indicator, is not much; it is around 1-2%. When a compression algorithm reaches its "full" potential it is hard to enhance it even more, so the 2% is much in high-rate compression where every bit counts.

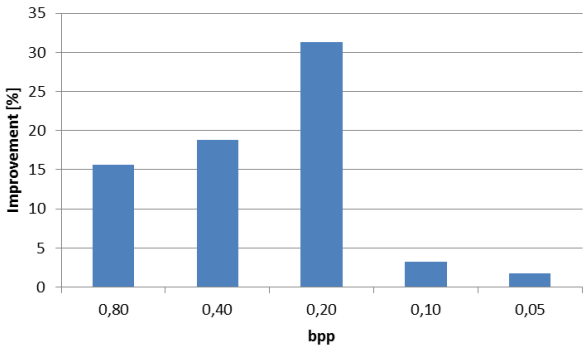

Fig. 16. EEDC-BTW versus EEDC improvement for image office

By observing the figures and tables we can conclude that the introduction of a Burrows-Wheeler transform to model the input data for the range coder yielded good results. Within the same number of bytes we managed to insert more pixels that are crucial to image reconstruction, i.e. image interpolation. The more pixels we have stored, the reconstructed image quality will be better.

We came to conclusion that the EEDC-BWT and EEDC are more efficient in images that lack high detail, i.e. images that have clearly stated borders and large gradient filled areas. The EEDC-BWT introduced in this article made a little step towards compression of images that have high detail areas which is a vast improvement.

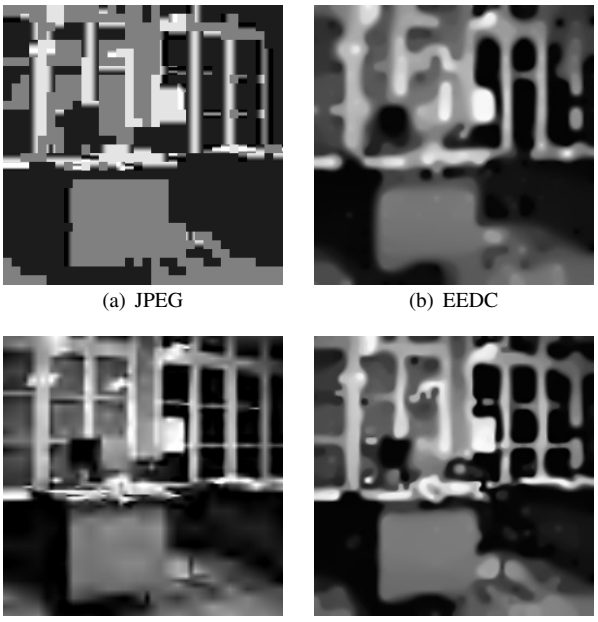

(a) JPEG (b) EEDC

(c) JPEG2000 (d) EEDC-BWT

Fig. 17. Office image compression

The computational complexity of the proposed method is a weak link since it uses a block sorting algorithm (BWT). The JPEG and JPEG 2000 perform almost in real time while the EEDC-BWT needs around 15 seconds for coding and decoding.

Presented results show that there are further EEDC modifications possible which open new challenges for high rate compression.

ACKNOWLEDGEMENTS

Irena Galić would like to thank Joachim Weickert, Martin Welk and Andrés Bruhn for interesting discussions on EED-based interpolation during her stay at the Saarland University, Germany.

[1] M. Bertalmío, G. Sapiro, V. Caselles, C. Ballester, "Image inpainting", In Proc. SIGGRAPH 2000, pp. 417–424, July 2000.

[2] V. Caselles, J.-M. Morel, and C. Sbert "An axiomatic approach to image interpolation", IEEE Transactions on Image Processing, 7(3): pp. 376–386, March 1998.

[3] P. Charbonnier, L. Blanc-Féraud, G. Aubert, and M. Barlaud, "Deterministic edge-preserving regularization in computed imaging". IEEE Transactions on Image Processing, 6(2): pp. 298–311, 1997.

[4] R. Distasi, M. Nappi, and S. Vitulano, "Image compression by B-tree triangular coding", IEEE Transactions on Communications, 45(9), pp. 1095 – 1100, September 1997.

[5] J. Duchon, "Interpolation des fonctions de deux variables suivant le principe de la flexion des plaques minces", RAIRO Mathematical Models and Methods in the Applied Sciences, 10, pp. 5–12, 1976.

[6] I. Galić, J. Weickert, M. Welk, A. Bruhn, A. Belyaev, H-P, Seidel, "Image Compression with Anisotropic Diffucion", Journal of Mathematical Imaging and Vision, vol. 31, num. 2-3, pp. 255–269. 2008.

[7] I. Galić, J. Weickert, M. Welk, A. Bruhn, A. Belyaev, and H.-P. Seidel, "Towards PDE-based image compression", In N. Paragios, O. Faugeras, T. Chan, and C. Schnörr, (eds.), Variational, Geometric and Level-Set Methods in Computer Vision, vol. 3752 of Lecture Notes in Computer Science, pp. 37–48. Springer, Berlin, 2005.

[8] T. Iijima, "Basic theory on normalization of pattern (in case of typical one-dimensional pattern)", Bulletin of the Electrotechnical Laboratory, 26:, pp. 368–388, 1962. In Japanese.

[9] Č. Livada, I. Galić, B. Zovko-Cihlar, "EEDC Image Compression Using Burrows-Wheeler Data Modeling", Proc. Of 54th International Symposium ELMAR-2012, pp. 1-7, 2012.

[10] M. Mainberger and J. Weickert, "Edge-Based Image Compression with Homogeneous Diffusion", In Computer Analysis of Images and Patterns, Proc. 13th International Conference CAIP 2009, Münster, Germany, September 2009 - X. Jiang, N. Petkov (Eds.) Lecture Notes in Computer Science, vol. 5702, pp.476–483, Springer, Berlin, 2009.

[11] G. Manzini, "An analysis of the Burrows-Wheeler transform", Journal of the ACM, 48(3), pp. 407–430, May, 2001.

[12] W. B. Pennebaker and J. L. Mitchell, "JPEG: Still Image Data Compression Standard", Springer, New York, 1992.

[13] P. Perona, J. Malik, "Scale space and edge detection using anisotropic diffusion", Proc. IEEE Comp. Soc. Workshop on Computer Vision (Miami Beach, Nov. 30 – Dec. 2, 1987), IEEE Computer Society Press, Washington, 16–22, 1987.

[14] I. M. Pu, "Fundamental Data Compression", Butterworth-Heinemann, 2005M. Bertalmío, G. Sapiro, V. Caselles, C. Ballester, "Image inpainting", In Proc. SIGGRAPH 2000, pp. 417–424, July 2000.

[15] C. Schmaltz, J. Weickert and A. Bruhn, "Beating the quality of JPEG 2000 with anisotropic diffusion", In: Denzler, J., Notni, G., K.P. Subbalakshmi, "Lossless Image Compression", Lossless Compression Handbook, Academic Press, 9, pp. 207–226., 2003.

[16] D. S. Taubman and M. W. Marcellin, editors. "JPEG 2000: Image Compression Fundamentals", Standards and Practice. Kluwer, Boston, 2002.

[17] J. Weickert, "Anisotropic Diffusion in Image Processing", Teubner, Stuttgart, 1998.

[18] M. J. Weinberger, "Sequential prediction and ranking in universal context modeling and data compression", IEEE Transactions on Information Theory, 43(5), pp. 1697–1703, September, 1997.

[19] Y.-L. You and M. Kaveh. "Fourth-order partial differential equations for noise removal", IEEE Transactions on Image Processing, 9(10):1723–1730, October 2000.

Irena Galić received the M.Sc. degree in computer science from Universität des Saarlandes, Saarbrücken, Germany, in 2004, and PhD. degree in electrical engineering from Faculty of Electrical Engeneering, Osijek, Croatia, in 2011. She is curently assistant professor in the Department of Software Engineering, Faculty of Electrical Engeneering, Osijek, Croatia. Irena Galić performs research in image processing, computer vision and computer graphics, focusing on variational and PDE methods.

Časlav Livada was born in Osijek (Croatia) in 1985. He is currently assistant professor at Faculty of Electrical Engineering in Osijek, J.J. Strossmayer University. He received hid PhD degree from the J.J. Strossmayer University in 2013. where he is engaged in teaching and research. His primary interest covers image processing, 2D and 3D graphics and AI in game programming.

Branka Zovko-Cihlar received the PhD. degree in electrical engineering from Faculty of Electrical Engeneering, University of Zagreb, Zagreb, Croatia, in 1964. She is professor in the Department of Radiocommunications and Microwave Engineering, Faculty of Electrical Engineering and Computing, University of Zagreb. She has more than 35 years experience in television, broadcasting systems, and noise in radiocommunications. She has been the president of Croatian Council for Radio and Television. Prof. Zovko-Cihlar is the president of the Croatian Society of Electronics in Marine-ELMAR and a member of the Croatian Technical Academy.

AUTHORS' ADDRESSES

Assist. Prof. Irena Galić, PhD,
Assist. Prof. Časlav Livada, PhD,
Department of Software Engineering,
Visual Computing Group,
Faculty of Electrical Engineering,
J.J. Strossmayer University of Osijek,
Osijek, Croatia.
email: irena.galic@etfos.hr, caslav.livada@etfos.hr

Prof. Branka Zovko-Cihlar, PhD,
Department of Radiocomm. and Microwave Engineering,
Faculty of Electrical Engineering and Computing,
University of Zagreb,
Zagreb, Croatia.
email: branka.zovko-cihlar@fer.hr

Received: 2012-05-09
Accepted: 2016-03-18